

HOSTED BY

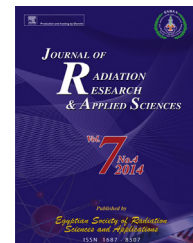


ELSEVIER

Available online at www.sciencedirect.com

ScienceDirect

Journal of Radiation Research and Applied Sciences

journal homepage: <http://www.elsevier.com/locate/jrras>

CrossMark

Thermoluminescence glow curve for UV induced ZrO₂:Ti phosphor with variable concentration of dopant and various heating rate

Neha Tiwari ^a, R.K. Kuraria ^a, Raunak Kumar Tamrakar ^{b,*}

^a Department of Physics, Govt. Autonomous Science College, Jabalpur, India

^b Department of Applied Physics, Bhilai Institute of Technology (Seth Balkrishan Memorial), Near Bhilai House, Durg (C.G.) 491001, India

ARTICLE INFO

Article history:

Received 30 August 2014

Accepted 8 September 2014

Available online 22 September 2014

Keywords:

Thermoluminescence

ZrO₂:Ti

Combustion synthesis

CGCD

Effect of dopant concentration

Various heating rate

ABSTRACT

The present paper reports the synthesis and characterization of Ti doped ZrO₂ nano-phosphors. The effects of variable concentration of titanium on thermoluminescence (TL) behaviour are studied. The samples were prepared by combustion a synthesis technique which is suitable for less time taking techniques also for large scale production for nano phosphors. The starting material used for sample preparation are Zr(NO₃)₃ and Ti(NO₃)₃ and urea used as a fuel. The prepared sample was characterized by X-ray diffraction technique (XRD) with variable concentration of Ti (0.05–0.5 mol%) there is no any phase change found with increase the concentration of Ti. Sample shows cubic structure and the particle size calculated by Scherer's formula. The surface morphology of prepared phosphor was determined by field emission gun scanning electron microscopy (FEGSEM) technique for optimized concentration of dopant. The good connectivity with grains and the semi-sphere like structure was found by FEGSEM. The functional group analysis was determined by Fourier transform infrared (FTIR) spectroscopic techniques. The prepared phosphor examined by thermoluminescence technique. For recording TL glow curve every time 2 mg phosphor was irradiated by UV 254 nm source and fixed the heating rate at 5 °C s⁻¹. Sample shows well resolved peak at 167 °C with a shoulder peak at 376 °C. The higher temperature peak shows the well stability and less fading in prepared phosphor. Also the effect of Ti concentration at fixed UV exposure time was studied. The effect of UV exposure time and dose versus intensity plot was studied. Sample shows linear response with dose and broaden peak with high temperature shows the more stability and less fading in TL glow curve. The linear dose response, high stability and less fading phenomenon shows the sample may be useful for thermoluminescence dosimetry application. Trapping parameters are calculated for every recorded glow curve. The prepared phosphor with optimized concentration of dopant was studied for various heating rate method. The various heating rate (3 °C s⁻¹ to 5 °C s⁻¹) shows shifting in TL glow peaks at higher temperature side. That is opposite behaviour shows in TL glow curve with various heating rate method. The presence of transition metal ions changes (Ti) the TL glow curve structure either enhancing or quenching the TL efficiency. These changes are a consequence of the crystalline field perturbation due to the different characteristics of the dopant ions which

* Corresponding author. Tel.: +91 9827850113.

E-mail addresses: tiwarineha1441@gmail.com, raunak.ruby@gmail.com, raunakphysics@gmail.com (R.K. Tamrakar).

Peer review under responsibility of The Egyptian Society of Radiation Sciences and Applications.

<http://dx.doi.org/10.1016/j.jrras.2014.09.006>

1687-8507/Copyright © 2014, The Egyptian Society of Radiation Sciences and Applications. Production and hosting by Elsevier B.V. All rights reserved.

supposedly replaces the Zr^{4+} sites. The traps and the glow curve structure are also dependent upon the morphology of the surface area which in turn depends on the nanocrystallite size. The nanocrystallite size depends also on the dopant ion. Furthermore, the obtained experimental results show that the presence of dopant ions also modifies the TL recombination efficiency which was found to be different for each irradiation type and the specific exposed material. It is important to notice that using the right dopant concentration, it is possible to maximize the TL efficiency and improve sensitivity and dose linearity for a specific irradiation type. For dual TL glow curve present in the sample it is very difficult to calculate the kinetic parameters from peak shape method. The kinetic parameters are calculated by (Computerized glow curve convolution technique) CGCD technique.

Copyright © 2014, The Egyptian Society of Radiation Sciences and Applications. Production and hosting by Elsevier B.V. All rights reserved.

1. Introduction

Due to their superior electrical, chemical and mechanical characteristics, nano range metal oxide based materials have great interest of research for researcher. Because this special property, they are widely used in lots of areas, such as lighting, LED, Solid state lighting, traffic signals, optical memory and luminous paint, etc (Conga, Lia, Leia, & Lia, 2007; Kowatari, Koyama, Satoh, Iinuma, & Uchida, 2002; Tamrakar, 2012, 2013; Tamrakar & Bisen, 2013). High optical transparency, low thermal conductivity, high pH stability, high melting point, high thermo mechanical resistance, high refractive index, low phonon energy, high chemical and photochemical stability are some requirement for the choosing a better host material to produce luminescence materials for different application. Zirconium oxide is have these qualities, which makes them promising candidates for host materials, and related studies have been reported (Meetei, Singh, & Sudarsan, 2012; Vidya et al. 2015; Zhang, Fu, Niu, & Xin, 2008).

ZrO_2 one of them very interesting material mainly due to its thermal stability and mechanical properties. On the other hand, it is claimed to be the only oxide catalyst that has acid, basic, reducing and oxidizing surface properties. It has the advantage of a high mechanical toughness and a thermal expansion coefficient closed to that of many metals, and can act as a reactive element (Meetei et al., 2012; Zhang et al. 2008). Recently, there are several reports on different kind luminescence from stress-activated $ZrO_2:Ti$, and intense visible light and afterglow were observed (Akiyama, Xu, & Nonaka, 2002; Chandra, 2010). But in over knowledge, no specific studies on thermoluminescence behaviour of $ZrO_2:Ti$ was done.

In this paper, we present a Ti doped ZrO_2 phosphor prepared by a traditional combustion synthesis method using urea as a fuel and characterized by X-ray diffraction technique for structural characterization. For morphological information, scanning electron microscope is used here. The Thermoluminescence (TL) glow curves of the Ti doped ZrO_2 phosphor, were measured with different minute of UV exposure time. For this, every time .2 mg phosphor was irradiated

by UV 254 nm source and optimized the heating rate of $5^\circ C s^{-1}$.

2. Experimental

2.1. Synthesis of $ZrO_2:Ti$ nanophosphor

The raw materials, zirconium (IV) oxynitrate hydrate ($ZrO(NO_3)_3 \cdot xH_2O$: 99.99%, (Sigma Aldrich) and Titanium(IV) nitrate tetrahydrate ($Ti(NO_3)_3 \cdot 4H_2O$ Sigma Aldrich) are the sources of Zr and Ti respectively. Urea was used as fuel. The stoichiometry of redox mixture used for combustion is calculated using total oxidizing and reducing valences of compounds (Tamrakar, Bisen, & Brahme, 2014; Tamrakar, Bisen, Upadhyay & Brahme, 2014).

For the synthesis of $ZrO_2:Ti$ (0.05–0.5 mol%), required amount of Urea and aqueous mixture of zirconium (IV) oxynitrate hydrate were subsequently added to the titanium nitrate solution while continuously stirring the mixture to ensure homogeneous mixing. The petri dish containing the heterogeneous redox mixture was introduced into a muffle furnace maintained at $500 \pm 10^\circ C$. Initially the solution boils and undergoes dehydration. Eventually the mixture undergoes decomposition, which results in the liberation of large amounts of gases (usually CO_2 , H_2O and N_2). This was followed by a spontaneous ignition which resulted in flame type combustion (Singanahally & Alexander, 2008, Tamrakar, Bisen, & Brahme, 2014). The whole process was completed in less than 5 min and a highly porous $ZrO_2:Ti$ nano powder was obtained. The prepared phosphors were used directly without and post heat treatment and directly subjected to further structural, morphological and luminescence studies.

2.2. Instrumental details

The final products were characterized using analytical X-pert PRO MPD X-ray diffractometer (PXRD) with copper k alpha anode of wavelength 1.5405 \AA . The diffraction patterns were recorded at room temperature with nickel filter in the 2θ range $15\text{--}85$ at a slow scan rate. The morphological features and particle size were studied by scanning electron microscopy

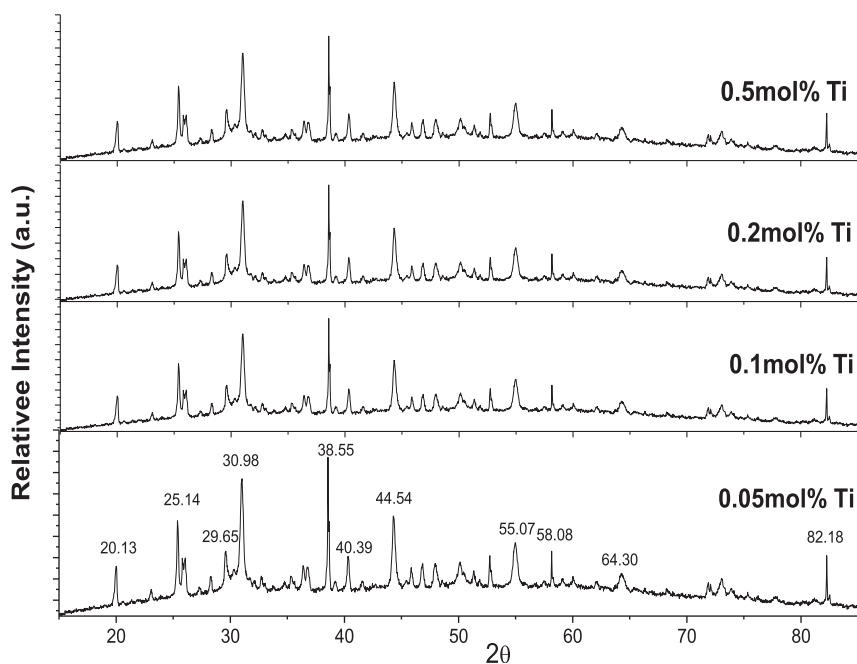


Fig. 1 – X-ray diffraction patterns of ZrO₂:Ti (0.05 to 0.5 mol%) Nanophosphor.

(SEM, Hitachi-3000). Thermally stimulated luminescence glow curves were recorded at room temperature by using TLD reader I1009 supplied by Nucleonix Sys. Pvt. Ltd. Hyderabad. (Dubey, Kaur, & Agrawal, 2010; Tamrakar, Kanchan & Bisen, 2014).

3. Results and discussion

3.1. X-ray diffraction results

For confirmation of prepared sample X-ray diffraction (XRD) characterization of the sample is done using Panalytical Xpert PRO MPD with copper k alpha anode of wavelength 1.5405 Å. Fig. 1 shows the PXRD patterns of ZrO₂:Ti (0.05–0.5 mol%), nanophosphors. The crystal structures and the phase purity of the materials were determined by X-ray diffraction (XRD). The as-formed ZrO₂:Ti prepared by low temperature solution combustion technique using urea as fuel shows pure cubic phase without any post calcinations and no traces of additional peaks from monoclinic/tetragonal phase were observed. The oxygen vacancies were considered to be responsible for the formation of the cubic phase.

In addition, it was clearly seen that with the increase of Ti concentration, the diffraction peak of samples are unchanged, there is no any phase change, peak shifting and line broadening found with increase the concentration of Ti. This is due to the lower concentration effect of Ti ions, which couldn't change the structure or the phase of the prepared phosphor. So, the sample shows cubic structure and the particle size calculated by Scherrer's formula. The Scherrer formula is given by: $D = 0.9 \lambda / \beta \cos \theta$, Where, D is the average particle size perpendicular to the reflecting planes, λ is the X-ray wavelength, β is the FWHM, and θ is the diffraction angle. The average particle size of prepared phosphor was 54 nm range.

3.2. Fourier transformation infrared spectroscopy (FTIR) results of ZrO₂:Ti (0.5 mol%) nanophosphor

Fig. 2 shows the FTIR spectra of combustion synthesized ZrO₂:Ti (0.5 mol%) phosphor. A strong absorption peak at 551.68 cm⁻¹ corresponds to Zr–O vibrational modes of ZrO₂ phase (Guo et al. 2009). The band at 743.85 attributed to the Eu–O stretching. Moreover, the absorption band centered at ≈ 3341.67 cm⁻¹ corresponds to OH stretching vibrations and peak centered at 1387.11 cm⁻¹ corresponds to bending vibration of O–H in H₂O (Tamrakar, Bisen, Robinson, Sahu & Brahme, 2014).

3.3. Scanning electron microscope results of ZrO₂:Ti (0.5 mol%) nanophosphor

The SEM micrographs of ZrO₂:Ti (0.5 mol%) nanophosphor show the crystallites with irregular shape and contain several voids and pores because of the escaping gases during combustion synthesis (Fig. 3). It can be observed that the

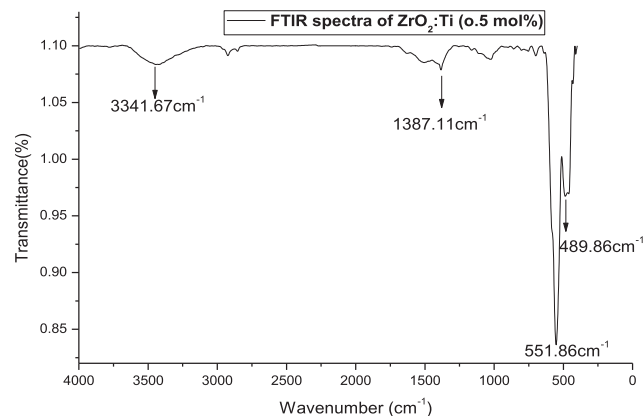


Fig. 2 – FTIR spectra of ZrO₂:Ti (0.5 mol%).

crystallites have no uniform shape and size. This was believed to be related to the non-uniform distribution of temperature and mass flow in the combustion flame. This type of porous network is a typical characteristic of combustion synthesized powders. The porous powders are highly friable which facilitates easy grinding to obtain finer particles. When the gas is escaping with high pressure pores are formed with the simultaneous formation of small particles near the pores (Tamrakar, Bisen, & Brahme, 2014).

3.4. Thermoluminescence studies of ZrO₂:Ti (0.05–0.5 mol%)

Thermoluminescence (TL) glow curves of ZrO₂:Ti phosphor were recorded after UV ray irradiation. The TL glow curves for different UV doses and for different Ti concentration at a heating rate of 5 °C s⁻¹ are shown in Fig. 4. For the variable concentration of Ti (0.05 mol% to 0.5 mol%) shows good TL glow curve at 167 °C. The peak position is fixed with variable concentration of Ti only TL intensity increases with increasing the concentration of dopant up to 0.2 mol% (Fig. 5) after that the relative TL intensity decreases due to concentration quenching occurs other reason is that the presence of transition metal ions changes (Ti) the TL glow curve structure either enhancing or quenching the TL efficiency. These changes are a consequence of the crystalline field perturbation due to the different characteristics of the dopant ions which supposedly replaces the Zr⁴⁺ sites. The traps and the glow curve structure are also dependent upon the morphology of the surface area which in turn depends on the nanocrystallite size (Tamrakar, Bisen, Sahu, and Brahme, 2014). The nanocrystallite size depends also on the dopant ion. Furthermore, the obtained experimental results show that the presence of dopant ions also modifies the TL recombination efficiency which was found to be different for each irradiation type and the specific exposed material. It is important to notice that using the right dopant concentration, it is possible to maximize the TL efficiency and improve sensitivity and dose linearity for a specific irradiation type (Tamrakar, Bisen, Sahu, and Brahme, 2014).

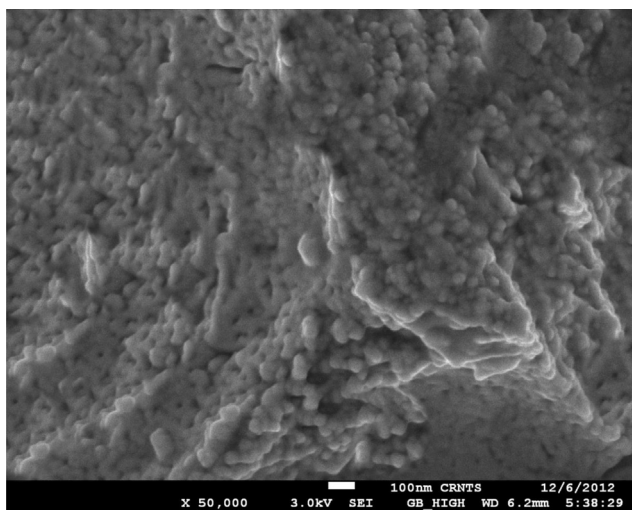


Fig. 3 – Scanning electron microscope image of ZrO₂:Ti (0.5 mol%).

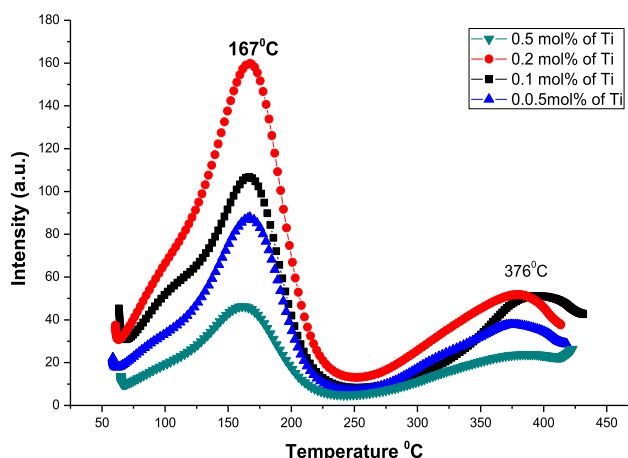


Fig. 4 – TL glow curve ZrO₂:Ti (0.05–0.5) for 20 min UV exposure time with Heating rate 5 °C s⁻¹.

The calculation of kinetic parameters such as activation energy (E) in eV as well as the frequency factor in s⁻¹ was determined by peak shape method. For the variation of dopant ion (Ti) the activation energy varies from 0.36 to 0.59 eV and the relative frequency factor found 8.2×10^4 to 5.6×10^7 s⁻¹. All peaks shows the first order of kinetic because the value of shape factor $\mu \sim 0.42$ or less than 0.42 (Table 1) shows the first order kinetics glow curve. Here the TL glow curve recorded for fixed UV exposure time 20 min as well as fixed heating rate 5 °C with variable concentration of Ti dopant.

TL glow curve recorded for optimized concentration of Ti (0.2 mol%) with the variation of UV exposure time shows resolved peak at 167 °C (Fig. 6). Here the relative TL intensity increases with increasing the UV exposure time and the optimized time of UV is 20 min UV exposure where maximum TL glow curve intensity was found. The sub linear response with dose it good property of TL glow curve. The variation with UV exposure time and relative TL intensity plot means dose versus intensity plot shows in Fig. 7. The heating rate used for recording of TL glow curve with variation of UV exposure time is fixed at 5 °C s⁻¹ so the behaviour displayed by TL glow curve is good. Here the shoulder peak with high temperature range

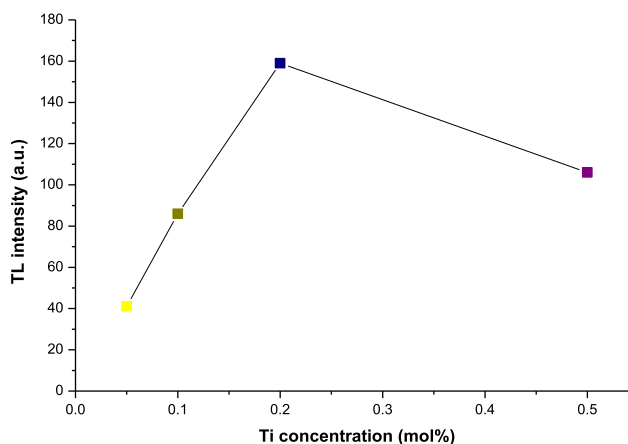
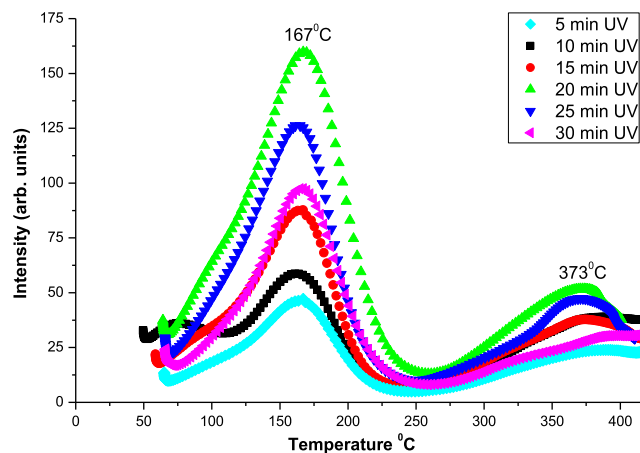


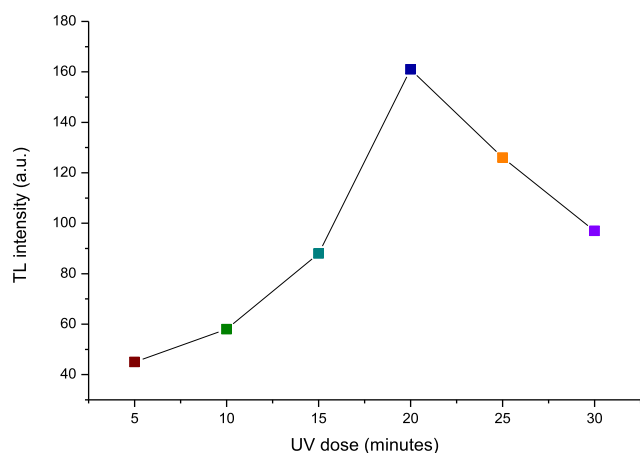
Fig. 5 – TL glow curve intensities ZrO₂:Ti % for 20 min UV exposure time with Heating rate 5 °C s⁻¹.

Table 1 – Kinetic parameters of $ZrO_2:Ti$ (0.05–0.5) for 25 min UV exposure time with Heating rate $6.7\text{ }^\circ\text{C s}^{-1}$ for 1st glow peak.

Ti concentration	T_1 ($^\circ\text{C}$)	T_m ($^\circ\text{C}$)	T_2 ($^\circ\text{C}$)	τ	δ	ω	$\mu = \delta/\omega$	Activation energy E in eV	Frequency factor S in s^{-1}
0.05%	115	167	193	52	26	78	0.333	0.452	1.1×10^{06}
0.1%	119	167	196	41	26	67	0.388	0.59	5.6×10^{07}
0.2%	119	167	196	48	29	77	0.377	0.498	4.2×10^{06}
0.5%	104	167	191	63	24	87	0.276	0.361	8.2×10^{04}

**Fig. 6 – TL glow curve of $ZrO_2:Ti(0.2\%)$ for different UV exposure time with heating rate $5\text{ }^\circ\text{C s}^{-1}$.**

373 $^\circ\text{C}$ shows the formation of more traps in the present sample $ZrO_2:Ti$ (0.2 mol%). When the number of traps formation occurs or the nature of dual peak concern it is very difficult to determine the kinetic parameters of the dual peak than we compare the kinetic parameter calculated by peak shape method in Fig. 6 and the computerized glow curve deconvoluted peak Fig. 10. Both the peak shows tremendous difference one is the first order of kinetics (Table 2) and one is non-first order of kinetic and varies from 1.4 to 2 (Table 4). So the exact kinetic parameter calculation was done by curve fitting technique or CGCD curve of TL glow curve.

**Fig. 7 – TL glow curve intensities for of $ZrO_2:Ti(0.2\%)$ for different UV exposure time with heating rate $5\text{ }^\circ\text{C s}^{-1}$.**

For the different heating rate method on TL glow curve shows the variation in peak temperature as well as the relative TL intensity (Fig. 8) of prepared phosphor for optimized concentration of dopant (Ti) i.e. 0.2 mol%. It shows the TL glow curve of ($3\text{--}5\text{ }^\circ\text{C s}^{-1}$) heating rate that means the various heating rate method support the TL glow curve. The TL glow curve shifts with increasing the heating rate and shifting occurs in higher temperature side (Fig. 9) opposite behaviour shows by TL glow curve same behaviour reported by dubey et al., (Dubey, Kaur, Agrawal, Suryanarayana, & Murth, 2014) in his recent article in natural sample. The corresponding value of the activation energy, order of kinetic and the frequency factor shows in Table 3. From Table 3 it is concluded that all three peak shows the first order of kinetic and the low value of activation energy (0.32–0.43 eV). The lower values of activation energy determine the less stability of phosphor for the optimized concentration of Ti in ZrO_2 host lattice. Less stability and high fading in TL glow curve shows the transition metal ion (Ti) behaves like a killer in the host matrix of ZrO_2 . But some time it enhances the luminescence efficiency as well as intensity. Again we compare the TL glow curve of prepared phosphor with various heating rate method and the CGCD curve of the prepared phosphor it is concluded that for the determination of kinetic parameters the CGCD technique is best.

TLD phosphor generally exhibits one or more peaks when the charge carriers (holes or electrons) were released. The dosimetric properties of TL materials largely depend on the kinetic parameters (E, b and s). These parameters will give valuable information about mechanism responsible for the emission in the phosphor. For a good TLD phosphor, a clear knowledge of its kinetic parameters was highly essential. These parameters can be estimated using Chen's set of empirical equations (Chen & Kirsh, 1981). For the peak shape method by deconvoluting the glow curve by using Glow curve deconvolution (Fig. 10). The peak shape method was generally called Chen's peak method which was used to determine the kinetic parameters of the glow peak of the TL materials. Frequency factor (s).

Once E and b are known, frequency factor (s) can be evaluated:

$$s = \frac{\beta E}{kT_m^2} \exp\left(\frac{E}{kT_m}\right) (1 + (b-1)\Delta_m^{-1})$$

where b is the linear heating rate, b the order of kinetics and $\Delta_m = \frac{2kT_m}{E}$

Order of kinetics.

To determine the order of kinetics (b), the form factor or symmetry factor is determined using the following expression:

Table 2 – Kinetic parameters of ZrO₂:Ti(2%) for different UV exposure time with Heating rate 5 °C s⁻¹ for 1st glow peak.

UV exposure time	T ₁ (°C)	T _m (°C)	T ₂ (°C)	τ	δ	ω	μ = δ/ω	Activation energy E in eV	Frequency factor S in s ⁻¹
5	118	167	193	49	26	75	0.347	0.484	2.8 × 10 ⁰⁶
10	118	167	194	49	27	76	0.355	0.485	2.5 × 10 ⁰⁶
15	119	167	192	48	25	73	0.342	0.494	3.7 × 10 ⁰⁶
20	119	167	196	48	29	77	0.377	0.498	4.2 × 10 ⁰⁶
25	124	167	188	43	21	64	0.328	0.554	2.1 × 10 ⁰⁷
30	125	167	198	42	31	73	0.425	0.581	4.3 × 10 ⁰⁷

Table 3 – Kinetic parameters of ZrO₂:Ti (0.2) for 20 min UV exposure with different heating rate in °C s⁻¹ for 1st glow peak.

Heating rate in °C/s	T ₁ (°C)	T _m (°C)	T ₂ (°C)	τ	δ	ω	μ = δ/ω	Activation energy E in eV	Frequency factor S in s ⁻¹
3	123	160	189	37	29	66	0.439	0.439	3.4 × 1008
4	99	164	192	65	28	93	0.301	0.322	1.9 × 1005
5	116	167	196	51	29	80	0.363	0.363	1.6 × 1006

Table 4 – Trapping parameters of a typical glow curve of ZrO₂:Ti(0.2%) for fixed 25 min UV exposure time with heating rate 5 °C s⁻¹.

Peaks	T ₁ (K)	T _m (K)	T ₂ (K)	μ _g	β	E (eV)	S (s ⁻¹)
Peak 1	335	393	458	0.52	2.0	0.33	1.4 × 10 ⁰⁵
Peak 2	404	437	471	0.50	1.8	0.75	5.7 × 10 ⁰⁹
Peak 3	557	613	661	.46	1.4	0.46	7.9 × 10 ⁰⁷

$$\mu_g = \frac{T_2 - T_m}{T_2 - T_1}$$

This involves calculation of T₁ and T₂. T₁ and T₂ are the temperatures corresponding to half of the maximum intensities on either side of the glow peak maximum temperature (T_m). The nature of the kinetics can be found by the form factor. Theoretically the value of geometrical form factor (μ_g) is close to 0.42 for first order kinetics, and value is 0.52 for second order kinetics (Dubey, Tiwari, et al., 2014, Tamrakar, Bisen, Sahu, and Brahme, 2014).

The estimated kinetic parameters for ZrO₂ Ti phosphor is calculated by curve fitting techniques CGCD curve of

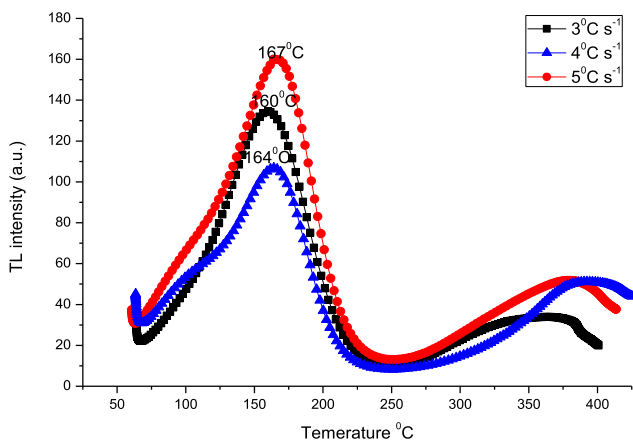


Fig. 8 – TL glow curve of ZrO₂:Ti (0.2%) for 20 min UV exposure with different heating rate in °C s⁻¹ for 1st glow peak.

experimental data and the peak shape method proposed by Chen and others (Chen, 1969; Chen & Kirsh, 1981, Kitis, Gomez-Ros, & Tuyn, 1998, Puchalska & Bilski, 2006, Tamrakar, Bisen, Sahu, and Brahme, 2014). The activation energy is found in between 0.33 and 0.75 eV and the frequency factor is range of 1.4 × 10⁰⁵ to 5.7 × 10⁰⁹ for UV irradiated phosphor.

4. Conclusion

The samples were prepared by combustion a synthesis technique which is suitable for less time taking techniques also for large scale production for nano phosphors. There is no any phase change found with increase the concentration of Ti. Sample shows cubic structure and the particle size calculated by Scherer's formula shows 54 nm. The good connectivity with grains and the semi-sphere line structure was found by FEG-SEM. Phosphor was irradiated by UV 254 nm source and fixed the heating rate at 5 °C s⁻¹. Sample shows well resolved peak at 167 °C with a shoulder peak at 376 °C. The higher temperature peak shows the well stability and less fading in prepared phosphor. Sample shows linear response with dose and broaden peak with high temperature shows the more stability

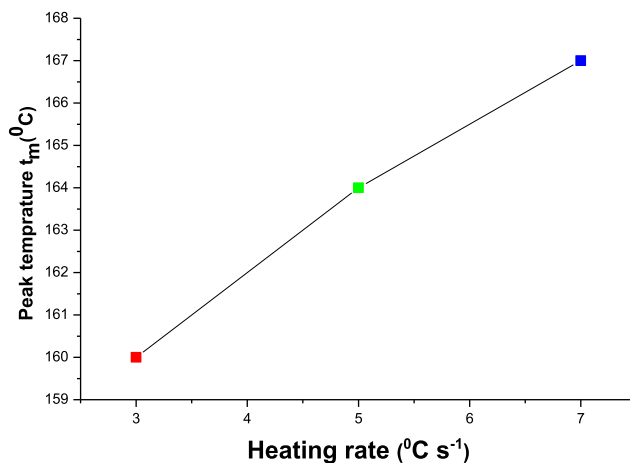


Fig. 9 – Heating rate vs peak temperature of ZrO₂:Ti (0.2%) for 20 min UV exposure with different heating rate in °C s⁻¹ for 1st glow peak.

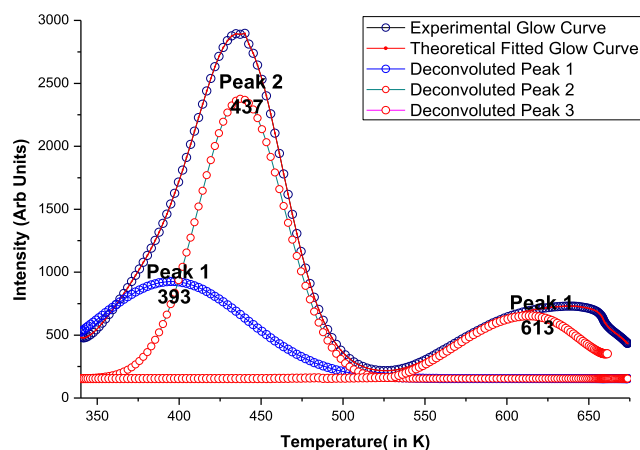


Fig. 10 – CGCD curve of experimental TL glow peak of $\text{ZrO}_2\text{:Ti}(0.2\%)$ for fixed 25 min UV exposure time with heating rate $5\text{ }^\circ\text{C s}^{-1}$.

and less fading in TL glow curve. The linear dose response, high stability and less fading phenomenon shows the sample may be useful for thermoluminescence dosimetry application. Trapping parameters are calculated for every recorded glow curve. The prepared phosphor with optimized concentration of dopant was studied for various heating rate method. The various heating rate ($3\text{ }^\circ\text{C s}^{-1}$ to $5\text{ }^\circ\text{C s}^{-1}$) shows shifting in TL glow peaks at higher temperature side. That is opposite behaviour shows in TL glow curve with various heating rate method. The presence of transition metal ions changes (Ti) the TL glow curve structure either enhancing or quenching the TL efficiency. These changes are a consequence of the crystalline field perturbation due to the different characteristics of the dopant ions which supposedly replaces the Zr^{4+} sites. The traps and the glow curve structure are also dependent upon the morphology of the surface area which in turn depends on the nanocrystallite size. The nanocrystallite size depends also on the dopant ion. Furthermore, the obtained experimental results show that the presence of dopant ions also modifies the TL recombination efficiency which was found to be different for each irradiation type and the specific exposed material. It is important to notice that using the right dopant concentration, it is possible to maximize the TL efficiency and improve sensitivity and dose linearity for a specific irradiation type. For dual TL glow curve present in the sample it is very difficult to calculate the kinetic parameters from peak shape method. The kinetic parameters are calculated by (Computerized glow curve convolution technique) CGCD technique and activation energy is found in between 0.33 and 0.75 eV and the frequency factor is range of 1.4×10^{05} to 5.7×10^{09} for UV irradiated phosphor.

REFERENCES

- Akiyama, M., Xu, C. N., & Nonaka, K. (2002). Intense visible light emission from stress-activated $\text{ZrO}_2\text{:Ti}$. *Applied Physics Letters*, 81, 457. [http://dx.doi.org/10.1063/1, 1494463](http://dx.doi.org/10.1063/1.1494463).
- Chandra, B. P. (2010). Persistent mechanoluminescence induced by elastic deformation of $\text{ZrO}_2\text{:Ti}$ phosphors. *Journal of Luminescence*, 130, 2218–2222.
- Chen, R. (1969). On the calculation of activation energies and frequency factors from glow curves. *Journal of Applied Physics*, 40, 570–585.
- Chen, R., & Kirsh, Y. (1981). *The analysis of thermally stimulated processes*. Oxford, New York: Pergamon Press.
- Conga, Y., Lia, B., Leia, B., & Lia, W. (2007). Long lasting phosphorescent properties of Ti doped ZrO_2 . *Journal of Luminescence*, 126, 822–826.
- Dubey, V., Kaur, J., Agrawal, S., & Suryanarayana, N. S. (2010). Kinetics of TL glow peak of limestone from Patharia of CG Basin (India). *Jour. Miner. Mater. Charac. Engin.*, 9(12), 1101–1111.
- Dubey, V., Kaur, J., Agrawal, S., Suryanarayana, N. S., & Murthy, K. V. R. (2014). Thermoluminescence study, including the effect of heating rate, and chemical characterization of Amarnath stone collected from Amarnath Holy Cave. *Research on Chemical Intermediates February*, 40(2), 531–536.
- Dubey, V., Tiwari, R., Pradhan, M. K., Rathore, G. S., Sharma, C., & Tamrakar, R. K. (2014). Photoluminescence and thermoluminescence Behavior of $\text{Zn}_2\text{SiO}_4\text{:Mn}^{2+}, \text{Eu}^{2+}$ Phosphor. Columbia International Publishing. *Journal of Luminescence and Applications*, 1(1), 30–39.
- Guo, L. M., Zhao, J. L., Wang, X. X., Xu, R. Q., Lu, Z. M., & Li, Y. X. (2009). Bioactivity of zirconia nanotube arrays fabricated by electrochemical anodization. *Materials Science and Engineering: C* 29, 1174–1177.
- Kitis, G., Gomez-Ros, J. M., & Tuyn, J. W. N. (1998). Thermoluminescence glow-curve deconvolution functions for first, second and general orders of kinetics. *Journal of Physics D: Applied Physics*, 31, 2636–2641.
- Kowatari, M., Koyama, D., Satoh, Y., Iinuma, K., & Uchida, S. (21 March 2002). The temperature dependence of luminescence from a long-lasting phosphor exposed to ionizing radiation. *Nuclear Instruments and Methods in Physics Research Section A: Accelerators, Spectrometers, Detectors and Associated Equipment*, 480(2–3), 431–439.
- Meetei, S. D., Singh, S. D., & Sudarsan, V. (February 2012). Polyol synthesis and characterizations of cubic $\text{ZrO}_2\text{:Eu}^{3+}$ nanocrystals. *Journal of Alloys and Compounds*, 514(15), 174–178.
- Puchalska, M., & Bilski, P. (July 2006). 2006. GlowFit—a new tool for thermoluminescence glow-curve deconvolution. *Radiation Measurements*, 41(6), 659–664.
- Singanaahally, T. A., & Alexander, S. M. (2008). Combustion synthesis and nanomaterials. *Current Opinion in Solid State and Materials Science*, 12, 44–50.
- Tamrakar, R. K. (2012). *Studies on absorption spectra of Mn doped CdS nanoparticles*. LAP Lambert Academic Publishing, VerlAg, ISBN 978-3-659-26222-7.
- Tamrakar, R. K. (2013). UV-Irradiated thermoluminescence studies of bulk CdS with trap parameter. *Research on Chemical Intermediates*. [10.1007/s11164-013-1166-4](https://doi.org/10.1007/s11164-013-1166-4).
- Tamrakar, R. K., & Bisen, D. P. (2013). Optical and kinetic studies of CdS: Cu nanoparticles. *Research on Chemical Intermediates*, 39, 3043–3048.
- Tamrakar, R. K., Bisen, D. P., & Brahme, N. (2014). Characterization and luminescence properties of Gd_2O_3 phosphor. *Research on Chemical Intermediates*, 40, 1771–1779.
- Tamrakar, R. K., Bisen, D. P., Robinson, C. S., Sahu, I. P., & Brahme, N. (2014). Ytterbium doped Gadolinium oxide ($\text{Gd}_2\text{O}_3\text{:Yb}^{3+}$) phosphor: topology, morphology, and luminescence behaviour in Hindawi Publishing Corporation. *Indian Journal of Materials Science*, 2014, 7. Article ID 396147.
- Tamrakar, R. K., Bisen, D. P., Sahu, I. P., & Brahme, N. (201430 July). UV and gamma ray induced thermoluminescence properties of cubic $\text{Gd}_2\text{O}_3\text{:Er}^{3+}$ phosphor. *Journal of Radiation Research and Applied Sciences*. <http://dx.doi.org/10.1016/j.jrras.2014.07.003>.

- Tamrakar, R. K., Bisen, D. P., Upadhyay, K., & Bramhe, N. (2014). Effect of fuel on structural and optical characterization of $Gd_2O_3:Er^{3+}$ phosphor. *Journal of Luminescence and Applications*, 1(1), 23–29.
- Tamrakar, R. K., Kanchan, U., & Bisen, D. P. (2014). Gamma ray induced thermoluminescence studies of yttrium (III) oxide nanopowders doped with gadolinium. *Journal of Radiation Research and Applied Sciences*. <http://dx.doi.org/10.1016/j.jrras.2014.08.012>.
- Vidya, Y. S., Anantharaju, K. S., Nagabhushana, H., Sharma, S. C., Nagaswarupa, H. P., Prashantha, S. C., et al. (January 2015). Combustion synthesized tetragonal $ZrO_2:Eu^{3+}$ nanophosphors: structural and photoluminescence studies. *Spectrochimica Acta Part A: Molecular and Biomolecular Spectroscopy*, 135(25), 241–251.
- Zhang, H., Fu, X., Niu, S., & Xin, Q. (2008). Blue emission of $ZrO_2:Tm$ nanocrystals with different crystal structure under UV excitation. *Journal of Non-Crystalline Solids*, 354(14), 1559–1563.